JPn Neuroscience

The Journal of Physiology

J Physiol 592.7 (2014) pp 1519–1534

Peripherally driven low-threshold inhibitory inputs to lamina I local-circuit and projection neurones: a new circuit for gating pain responses

Liliana L. Luz[1], Peter Szucs[1,2,3] and Boris V. Safronov[1]

[1]*Neuronal Networks Group, Institute of Molecular and Cellular Biology (IBMC) and* [2]*Laboratory of Cellular and Molecular Biology, Faculty of Medicine, University of Porto, Porto, Portugal and* [3]*Department of Physiology, University of Debrecen, Debrecen, Hungary*

Key points

- Spinal lamina I is a key element of the pain processing system which relays peripheral inputs to supraspinal areas.
- In this study, we focused on signal processing in identified lamina I local-circuit and projection neurones in their functionally preserved network in an isolated spinal cord preparation.
- We found that local-circuit neurones generate spontaneous rhythmic firing, which persists in the presence of blockers of fast synaptic transmission.
- We describe a novel, low-threshold, primary afferent-driven inhibitory input to lamina I neurones, which temporally preceded classical high-threshold excitatory inputs and may function as a postsynaptic gate controlling pain.
- One-third of local-circuit neurones and two-thirds of projection neurones responded to substance P application.
- These results help us understand the role of lamina I neurones in a new circuit for gating pain responses.

Abstract Spinal lamina I is a key element of the pain processing system which relays primary afferent input to supraspinal areas. However, little is known about how the signal is modulated by its intrinsic network including local-circuit neurones (LCNs) and much less numerous anterolateral tract projection neurones (PNs). Here, we used whole-cell patch clamp recordings in an isolated spinal cord preparation to examine properties of identified LCNs ($n = 85$) and PNs ($n = 73$) in their functionally preserved local networks. Forty LCNs showed spontaneous rhythmic firing (2–7 Hz) at zero current injection, which persisted in the presence of blockers of fast synaptic transmission. In the remaining cases, most LCNs and PNs fired tonically in response to depolarizing current injections. We identified LCNs and PNs receiving low-threshold primary afferent-driven inhibitory inputs, which in many cases were disynaptic and temporally preceded classical high-threshold excitatory inputs. This direct inhibitory link between low-threshold afferents and PNs can function as a postsynaptic gate controlling the nociceptive information flow in the spinal cord. The LCNs were found to be integrated into the superficial dorsal horn network by their receipt of monosynaptic and disynaptic inputs from other lamina I and II neurones. One-third of LCNs and two-thirds of PNs tested responded to substance P application. Thus, substance P released by a noxious afferent stimulation may excite PNs in two ways: directly, and via the activation of presynaptic LCN circuitries. In conclusion, we have described important properties of identified lamina I neurones and their roles in a new circuit for gating pain responses.

L. L. Luz and P. Szucs contributed equally to this work.

DOI: 10.1113/jphysiol.2013.269472

(Resubmitted 6 December 2013; accepted after revision 6 January 2014; first published online 13 January 2014)
Corresponding author B. V. Safronov: Neuronal Networks Group, Instituto de Biologia Molecular e Celular (IBMC), Universidade do Porto, Rua do Campo Alegre 823, 4150–180 Porto, Portugal. Email: safronov@ibmc.up.pt

Abbreviations ACSF, artificial cerebrospinal fluid; CV, conduction velocity; LCNs, local-circuit neurones; NK1Rs, neurokinin 1 receptors; PNs, projection neurones; RMP, resting membrane potential

Introduction

Spinal lamina I is a key element of the pain processing system which relays primary afferent input to specific areas of the brainstem and thalamus (Willis & Coggeshall, 1991). It contains numerous local-circuit neurones (LCNs) and a small population (~5%) of projection neurones (PNs) (Bice & Beal, 1997; Spike *et al.* 2003; Todd & Koerber, 2006). Lamina I neurones show diverse firing properties (Grudt & Perl, 2002; Prescott & De Koninck, 2002; Ruscheweyh *et al.* 2004), which determine how synaptic excitation is converted into trains of action potentials (Lopez-Garcia & King, 1994; Graham *et al.* 2004) and set rhythmic network activity necessary for the development of spinal sensory circuitries (Li & Baccei, 2011). However, these firing properties have not yet been studied by tight-seal recording in identified LCNs and PNs in a preparation that preserves their entire dendritic and axonal architecture.

According to the classical theory (Melzack & Wall, 1965), nociceptive transmission in the spinal cord is controlled by a gate, which can open and close depending on the relative balance of activity in large *versus* small afferents. Although the presynaptic inhibition of the latter was considered as a major mechanism of pain control, a possible contribution of some undetected postsynaptic mechanisms had not been ruled out (Melzack & Wall, 1965). Our recent observations, however, suggest there may be a straight postsynaptic inhibitory link between the low-threshold afferents and lamina I neurones. In isolated spinal cord, we observed an afferent-driven inhibition of lamina I neurones, which preceded monosynaptic high-threshold excitatory inputs [Szucs *et al.* 2009 (Fig. 3)]. This apparently disynaptic inhibition, which may act as a postsynaptic gate controlling the nociceptive information flow in lamina I LCNs or PNs, has not been investigated in detail.

Lamina I neurones are integrated in the superficial dorsal horn network (Lu & Perl, 2005; Graham *et al.* 2007; Santos *et al.* 2007, 2009; Kato *et al.* 2009; Todd, 2010). In addition, their axons form intersegmental, propriospinal and interlaminar connections, the last of which reach the ipsilateral ventral horn (Szucs *et al.* 2010, 2013). Anterolateral tract PNs receive monosynaptic inputs from lamina I LCNs, which can be wired via very long axodendritic pathways (Luz *et al.* 2010). However, less is known about local inputs to LCNs.

Peptide substance P is released from the central terminals of nociceptive primary afferent neurones following noxious stimulation (Duggan *et al.* 1987; Mantyh *et al.* 1995) and acts in lamina I on neurokinin 1 receptors (NK1Rs) expressed in excitatory LCNs (Littlewood *et al.* 1995; Al Ghamdi *et al.* 2009) and in 80% of PNs (Marshall *et al.* 1996; Todd *et al.* 2000; Al-Khater *et al.* 2008). Although the majority of NK1R-expressing neurones in lamina I are LCNs (Al Ghamdi *et al.* 2009), we know little about their responsiveness to substance P.

This work examined the intrinsic firing properties, low-threshold afferent-driven inhibition, local connectivity and substance P responses of identified lamina I neurones in an isolated spinal cord preparation.

Methods

Ethical approval

Laboratory Wistar rats (P14–P21) were killed by decapitation in accordance with national guidelines (Direcção Geral de Veterinária, Ministério da Agricultura) after anaesthesia with I.P. injection of Na^+-pentobarbital (30 mg kg^{-1}) and a subsequent check for lack of pedal withdrawal reflexes. The experiments were carried out according to the guidelines laid down by the study institution's animal welfare committee (Comissão de Ética do Instituto de Biologia Molecular e Celular).

Preparation

The vertebral column was quickly cut out and immersed in oxygenated artificial cerebrospinal fluid (ACSF) at room temperature. The lumbar spinal cord was dissected and the pia mater in the region of interest was removed with forceps and scissors to provide access to the recording pipettes. The spinal cord was glued with cyanoacrylate adhesive to a gold plate (with the dorsolateral surface facing upwards) and transferred to the recording chamber. All measurements were made at 22–24°C. Lamina I neurones were visualized through the intact white matter using the oblique infrared light-emitting diode illumination technique (Safronov *et al.* 2007; Szucs *et al.* 2009) in the region between the dorsolateral funiculus and the dorsal root entry zone (Pinto *et al.* 2010). Lamina I neurones could be clearly distinguished from the more deeply

located lamina II neurones, the somata of which were smaller and which were densely packed within their layer (Szucs *et al.* 2010). All lamina I neurones described here were proven to be either LCNs or PNs by *post hoc* analysis of their axon structure. The axons of LCNs branched densely within the ipsilateral dorsal horn and never had any branch crossing the spinal cord midline, whereas those of PNs entered the contralateral anterolateral tract.

Recording

Recordings from lumbar (L1–6) lamina I neurones were performed in the whole-cell mode. ACSF contained 115 mM NaCl, 3 mM KCl, 2 mM $CaCl_2$, 1 mM $MgCl_2$, 1 mM NaH_2PO_4, 25 mM $NaHCO_3$ and 11 mM glucose (bubbled with 95% O_2/5% CO_2). The pipettes were pulled from thick-walled glass (BioMedical Instruments GmbH, Zöllnitz, Germany) and fire-polished (resistance: 4–5 MΩ). The pipette solution contained 3 mM KCl, 150 mM K-gluconate, 1 mM $MgCl_2$, 1 mM BAPTA, 10 mM Hepes [pH 7.3 adjusted with KOH; final $[K^+]$: 160 mM] and 0.5–1% biocytin (calculated reversal potential for Cl^- was −82 mV). In 17 cases (nine LCNs and eight PNs recorded in voltage-clamp mode), the effect of substance P was studied using a pipette solution containing 120 mM KCl, 15 mM NaCl, 1 mM $MgCl_2$, 10 mM EGTA, 10 mM Hepes [pH 7.3 adjusted with KOH; final $[K^+]$: 150 mM] and 0.5–1% biocytin. The amplifier was an EPC10-Double (HEKA Elektronik GmbH, Lambrecht/Pfalz, Germany). The signal was low-pass filtered at 2.9 kHz and sampled at 10 kHz. Offset potentials were compensated before seal formation. Liquid junction potentials were calculated and corrected for in all experiments using the compensation circuitry of the amplifier. The blockers 6-cyano-7-nitroquinoxaline-2,3-dione (CNQX), strychnine and picrotoxin were purchased from Sigma-Aldrich Corp. (St Louis, MO, USA).

Input resistance (R_{IN}) was measured in current-clamp mode from a hyperpolarization evoked by an injection of a 500 ms current pulse of −10 pA to −20 pA. Resting membrane potential (RMP) was measured with a balanced amplifier input (Santos *et al.* 2004). Intrinsic firing patterns were classified as tonic, gap, burst or rhythmic, according to descriptions given for superficial dorsal horn neurones (Prescott & De Koninck, 2002; Melnick *et al.* 2004; Ruscheweyh *et al.* 2004; Li & Baccei, 2011). A tonic neurone was able to support regular discharge of action potentials during depolarization evoked by 500 ms current pulse injections. A gap neurone showed a long interval between the first two spikes in a train at strong stimulations; at weak stimulations, the first spike appeared with a typical delay. A burst neurone generated one or several bursts of two to four spikes each during tonic firing; the first burst appeared at the onset of depolarization. A rhythmic neurone continuously discharged action potentials at zero current injection; therefore RMP could not be determined for a cell from this group. Rhythmic neurones in our study corresponded to the 'tonic' and 'irregular' groups of spontaneously active lamina I neurones described by Li & Baccei (2011).

Primary afferent inputs were recorded in lamina I neurones located in segment L4. Two attached ipsilateral roots, L4 and L5, were stimulated via suction electrodes as described in Pinto *et al.* (2008*b*, 2010) using an isolated pulse stimulator (2100; A-M Systems, Inc., Sequim, WA, USA). The root lengths were 6–8 mm for the neurones described in Table 2. Each suction electrode had its own reference electrode; there was no cross-stimulation between roots. Pulses (50 μs or 100 μs) of increasing amplitude were applied to recruit Aδ fibres, and 1 ms pulses were applied to activate both Aδ and C fibres. Monosynaptic EPSCs were identified on the basis of low failure rates and small latency variations as described in Pinto *et al.* (2010). The afferent conduction velocity (CV) was calculated by dividing the conduction distance by the conduction time. The former included the length of the root from the opening of the suction electrode to the dorsal root entry zone and the estimated pathway within the spinal cord. The spinal pathway was measured from images taken after the recording session and calculated as the sum of the rostrocaudal and mediolateral distances between the cell body and the corresponding dorsal root entry zone. The spinal pathways for the cells in Table 2 were 0.3–1.4 mm for the L4 root and 0.9–2.5 mm for the L5 root. Conduction time for a monosynaptic EPSC was calculated from its latency with a 1 ms allowance for synaptic transmission. In the case of a disynaptic inhibition (via an intercalated neurone), allowance was made for two serial synaptic transmissions, from the primary afferent to the intercalated neurone (1 ms) and from the intercalated neurone to the recorded neurone (1 ms), as well as for the spike initiation in the intercalated neurone. Although initiation time varied considerably from cell to cell, we assumed it to be 2 ms, which corresponded to the fastest spike initiation observed in neurones with the strongest excitatory inputs (see Fig. 3*C*, left). For this reason, the total allowance of 4 ms in disynaptic transmission at 22–24°C should be considered as an underestimation and as giving the lower border estimate for the CV of conveying afferents. CVs of the Aδ and C fibres calculated for monosynaptic inputs in this study were in the range described by Pinto *et al.* (2008*a*).

Local monosynaptic inputs to LCNs from lamina I and lamina II neurones were identified as described (Santos *et al.* 2009; Luz *et al.* 2010). In experiments using substance P (Sigma-Aldrich Corp.), the lumbar spinal cord was cut into two or three blocks, each containing at least two complete segments. In each block, the drug was applied only once in order to avoid a possible receptor

Table 1. Intrinsic membrane properties and responsiveness to substance P in local-circuit neurones (LCNs) and projection neurones (PNs)

	LCNs				PNs			
	n	RMP in mV	R_{IN} in GΩ	SP	*n*	RMP in mV	R_{IN} in GΩ	SP
Total	85	n.a.*	0.97 ± 0.05 ($n = 84$)	15/41	73	−72.8 ± 0.9 ($n = 70$)	0.77 ± 0.05 ($n = 73$)	21/31
Tonic	27	−69.1 ± 1.2 ($n = 27$)	1.01 ± 0.06 ($n = 27$)	7/14	53	−72.6 ± 1.1 ($n = 51$)	0.77 ± 0.06 ($n = 53$)	18/25
Gap	7	−81.2 ± 2.9 ($n = 7$)	0.89 ± 0.05 ($n = 7$)	1/5	2	−82 and −88	0.66 and 1.71	1/2
Rhythmic	40	n.a.*	1.0 ± 0.08† ($n = 40$)	7/20	0			
Burst	0				7	−70.7 ± 1.6 ($n = 7$)	0.34 ± 0.07 ($n = 7$)	0/0
Unclassified	11	−62.9 ± 6.4 ($n = 6$)	0.81 ± 0.26 ($n = 10$)	0/2	11	−73.0 ± 2.0 ($n = 10$)	0.94 ± 0.2 ($n = 11$)	2/4

RMP, resting membrane potential; R_{IN}, input resistance; n.a., non-applicable. *The RMP could not be determined for rhythmic LCNs, and therefore, for the total LCN population. †In rhythmic LCNs, sustained hyperpolarizing current was first injected to stop the firing, and then additional hyperpolarizing current pulse was applied to measure R_{IN}. Unclassified, these neurones showed features typical for more than one group, or changed their firing pattern during recording. SP, substance P; the data for each cell group are presented as the number of responding/tested neurones; pooled data from voltage- and current-clamp experiments.

desensitization, and the neuronal response was recorded in either voltage- or current-clamp mode.

Histological processing and cell reconstruction

After fixation in 4% paraformaldehyde, the spinal cord was embedded in agar and parasagittal serial sections of 100 μm thickness were prepared with a tissue slicer (VT 1000S; Leica Microsystems GmbH, Wetzlar, Germany). To reveal biocytin, sections were permeabilized with 50% ethanol and treated according to the avidin-biotinylated horseradish peroxidase method (ExtrAvidin-Peroxidase, diluted 1 : 1000; Sigma-Aldrich Corp.), followed by a diaminobenzidine chromogen reaction. Sections were counterstained with 1% toluidine blue and mounted in DPX (Fluka; Sigma-Aldrich Corp.). Photomicrographs were taken with a Primo Star microscope (Carl Zeiss Microscopy GmbH, Jena, Germany) equipped with a Guppy digital camera (Allied Vision Technologies GmbH, Stradtoda, Germany). The contrast and brightness of the images used for the figures were adjusted using Adobe Image Ready software. Distances were measured on the digital micrographs. Three-dimensional reconstructions of neurones in Fig. 4 were achieved as described in Szucs *et al.* (2013).

Unless otherwise stated, all data are given as the mean ± S.E.M. Parameters were compared using a paired or independent Student's *t* test. In Table 2, the variation in IPSC latency for disynaptic inhibition is described as S.D., σ_N.

Results

We recorded from and filled with biocytin 451 lamina I neurones, 158 of which were recovered to a degree that allowed their unequivocal identification as either LCNs ($n = 85$) or PNs ($n = 73$). These identified neurones form the basis of the present study.

Intrinsic firing properties of LCNs and PNs

Intrinsic firing properties were studied in a total of 85 LCNs and 73 PNs. Data are summarized in Table 1.

Twenty-seven LCNs fired tonically upon injection of depolarizing currents (Fig. 1*Aa*). Seven LCNs with a more negative RMP ($P < 0.001$) showed gap firing (Fig. 1*Ab*, left). In this group, R_{IN} measured at the RMP did not differ ($P = 0.88$) from that in the tonic group. If a gap-firing LCN was depolarized to about −70 mV by the steady-state current injection, its firing behaviour became tonic (Fig. 1*Ab*, right).

In 40 LCNs, rhythmic firing of spikes at frequencies of 2–7 Hz was observed at zero current injection (Fig. 1*Ac1*). The rhythmic firing could be stopped by an injection of hyperpolarizing current (−5 pA to −20 pA, $n = 10$) when membrane potential reached −70 mV to −80 mV. A rhythmic LCN discharged spikes at regular intervals (Fig. 1*Ac2*), which were influenced by spontaneous synaptic inputs (i.e. shortened by EPSPs and prolonged by IPSPs) (Fig. 1*Ac3*). The rhythmic firing persisted in the presence of a mixture of 10 μM CNQX, 100 μM picrotoxin and 1 μM strychnine (Fig. 1*Ac4*) blocking all spontaneous EPSPs and IPSPs ($n = 10$). Ion conductances underlying rhythmic firing in lamina I neurones have been described in detail by Li & Baccei (2011) and are outwith the scope of the present study.

The axon initial segment plays a crucial role in spike and pattern generation in dorsal horn neurones (Safronov *et al.* 1997). As it originates in many LCNs from primary dendrites (Szucs *et al.* 2013), we tested the hypothesis that the remote origin of the axon may be a specific feature of rhythmic LCNs. However, morphological analysis

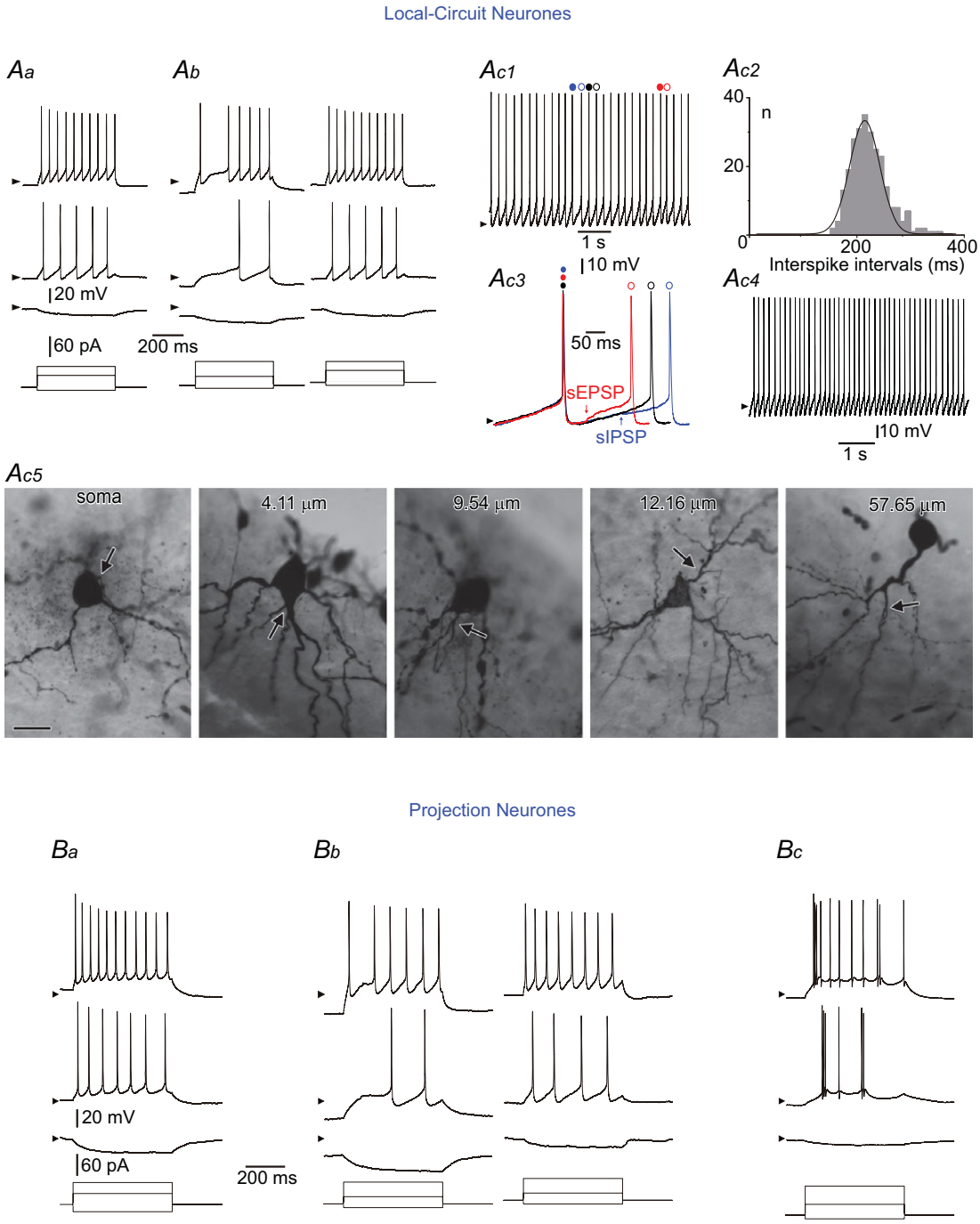

Figure 1. Intrinsic firing of local-circuit neurones (LCNs) and projection neurones (PNs)
Aa, a tonic LCN. *Ab*, a gap firing LCN. The stimulation protocol was applied to the neurone kept at its resting membrane potential (RMP) (left) and after sustained depolarization to −70 mV (right); note the change of firing pattern to tonic. *Ac1–4*, a rhythmic LCN. *Ac1*, intrinsic firing at zero current injection. Spikes indicated by coloured circles are shown superimposed in *Ac3*. *Ac2*, distribution of interspike intervals for the neurone shown in *Ac1* (bin width: 10 ms; 259 intervals analysed). Data are fitted with a Gaussian function (mean: 220 ms; σ, 29 ms). *Ac3*, interspike intervals: control (black), shortened by a spontaneous EPSP (sEPSP, red) and prolonged by a spontaneous IPSP (sIPSP, blue). *Ac4*, rhythmic firing in the presence of the mixture of 10 μM CNQX, 100 μM picrotoxin and 1 μM strychnine (in the neurone in *Ac1*). All spontaneous EPSPs and IPSPs were blocked. *Ac5*, somatic and dendritic origins of the axon initial segment in five different LCNs showing distances between the axon origin point and the soma. Scale bar: 25 μm. *Ba*, a tonic PN. *Bb*, a gap firing PN. The stimulation was applied to the neurone kept at its RMP (left) and after sustained depolarization to −70 mV (right). *Bc*, a burst firing PN. Stimulation protocols are shown below current-clamp recordings; arrowheads indicate a potential of −70 mV.

Table 2. Low-threshold inhibitory inputs to lamina I neurones

		Anatomy			Primary afferent-driven inhibition							
					Low-threshold short-latency IPSC						Low-threshold long-latency IPSC	
			Axon		L4 root			L5 root				
Cell	Firing type	Somatodendritic type (spines)	Origin	Description	+/–	Failures	Latency variation (S.D.)	+/–	Failures	Latency variation (S.D.)	L4 root +/–	L5 root +/–
LCNs in L4												
26–01–2012e34	Rhythmic	Multipolar (few)	Soma	Local axon only	+	6 of 22 (27.3%)	0.93 ms $n = 16$	–			–	–
27–01–2012e33	Tonic	Multipolar (few)	Dendrite (10 μm)	Local axon only	n.t.			+	1 of 22 (4.5%)	0.87 ms $n = 21$	n.t.	–
16–02–2012e32	u.c.	Multipolar (n.a.)	Soma	Local axon and strong branch running rostrally in the ipsilateral DLF	+	6 of 25 (24%)	0.65 ms $n = 19$	+	1 of 25 (4%)	0.79 ms $n = 24$	–	–
17–02–2012e33	Rhythmic	Flattened (very few)	Soma	Local axon only	–			+	3 of 23 (13%)	0.51 ms $n = 20$	–	–
PNs in L4												
16–12–2011e20	Tonic	Flattened (few)	Dendrite (15 μm)	Projection axon and one lateral collateral running rostrally in the ipsilateral DLF	–			n.t.			+	n.t.
23–12–2011e18	Burst	Flattened (few)	Soma	Projection axon and one ipsilateral ventral collateral	+	2 of 21 (9.5%)	0.43 ms $n = 19$	+	8 of 21 (38.1%)	2.35 ms $n = 13$	–	–
10–02–2012e32	Tonic	Flattened (n.a.)	Soma	Projection axon only	–			+	6 of 20 (30%)	1.11 ms $n = 14$	+	–
17–02–2012e32	Tonic	Flattened, lateral dendrites in DLF (very few)	Soma	Projection axon and one lateral collateral running rostrally in the ipsilateral DLF	–			+	8 of 19 (42.1%)	1.58 ms $n = 11$	+	–
29–02–2012e32	u.c.	Pyramidal (frequent)	Dendrite (14 μm)	Projection axon only	–			n.t.			+	n.t.

Intrinsic firing properties and anatomical characteristics of four local-circuit neurones (LCNs) and five projection neurones (PNs) receiving the low-threshold inhibitory inputs from at least one root. Firing type; u.c., unclassified. Somatodendritic type; n.a., non-applicable, in these neurones the number of spines could not be estimated. Axon; in the case of the dendritic origin of the axon the distance between the origin point and the soma is indicated; DLF, dorsolateral funiculus. Primary afferent-driven inhibition: + and –, presence and absence of low-threshold inhibition, respectively; n.t., not tested; S.D., standard deviation (σ_N). For low-threshold short-latency IPSCs, failure rates and latency variations are given. They were calculated for the fastest individual components of the IPSCs (see Fig. 2*C*). For low-threshold short-latency IPSCs, the estimated lower border of conduction velocity of the conveying primary afferents ranged from 2.7 m/s to 0.94 m/s ($n = 9$).

indicated that in this cell type the major axon can originate from both the soma and remote dendritic locations (Fig. 1*Ac5*).

The remaining 11 LCNs could not be classified on the basis of their firing properties. In addition, it should be noted that none of the LCNs in our sample showed burst firing.

The majority of the PNs were tonic ($n = 53$) (Fig. 1*Ba*). In two cases, PNs showed gap firing when stimulated from their RMP (Fig. 1*Bb*, left), but sustained membrane depolarization to −70 mV transformed the firing pattern to tonic (Fig. 1*Bb*, right). Burst firing behaviour was seen in seven PNs (Fig. 1*Bc*), in which R_{IN} values were significantly lower than in tonic ($P < 0.001$) and unclassified ($P = 0.008$) PNs. The remaining 11 PNs could not be classified, but none of them showed rhythmic firing.

Thus, both LCNs and PNs could be tonic or gap firing, whereas rhythmic and bursting patterns, in our sample, were observed in LCNs and PNs, respectively.

Afferent-driven inhibition of LCNs and PNs

Primary afferent inputs were recorded in 11 LCNs and 10 PNs located in the L4 segment. Segmental (L4) and the neighbouring caudal (L5) roots were stimulated as those with the strongest inputs to L4 lamina I neurones (Pinto *et al.* 2010). In four LCNs and five PNs, we observed a low-threshold afferent-driven inhibition that, in many cases, preceded the classical monosynaptic excitation. Intrinsic firing properties, anatomical features and the low-threshold afferent-driven inhibition of these neurones are described in Table 2.

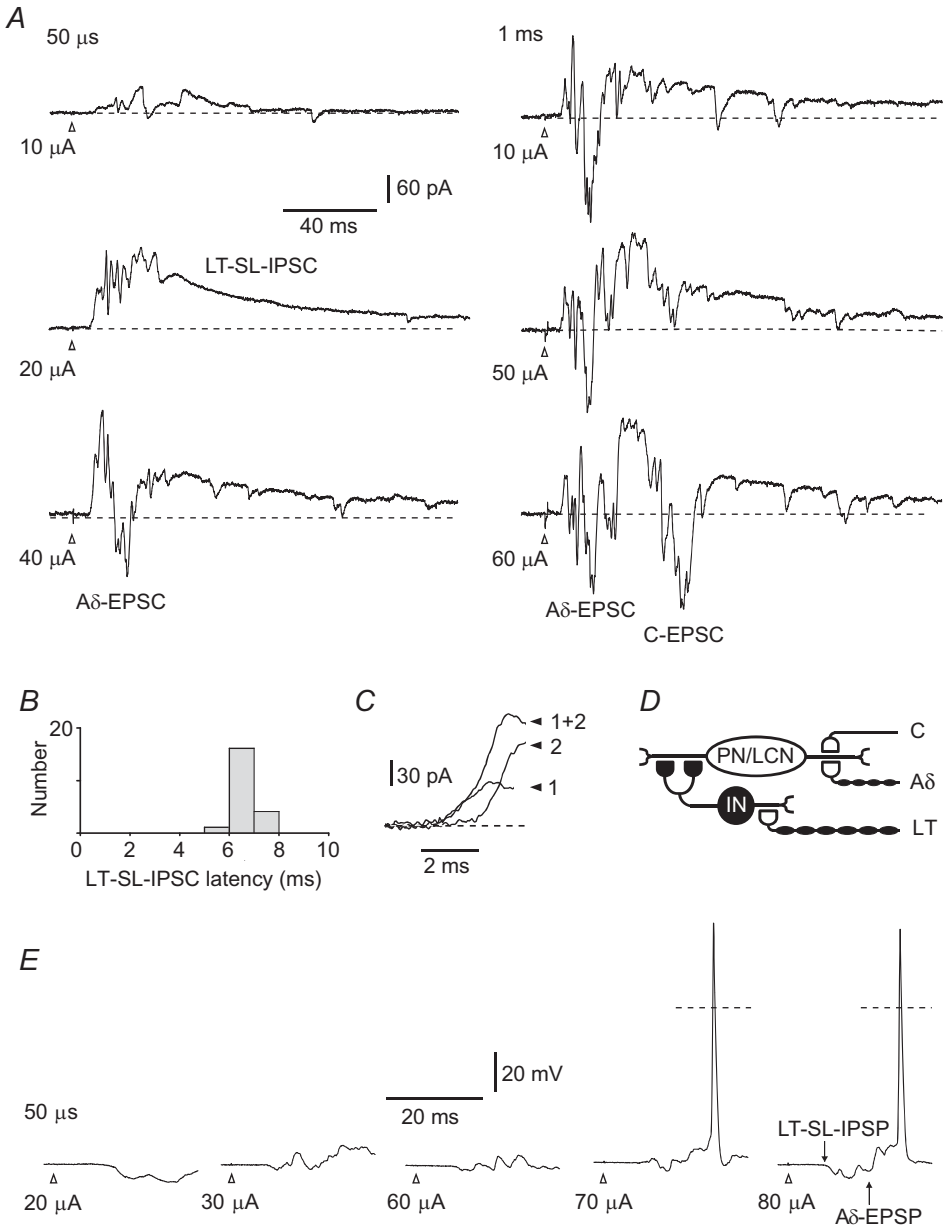

Figure 2. Low-threshold short-latency afferent-driven disynaptic inhibition
Synaptic inputs to a local-circuit neurone (LCN) located in segment L4 receiving inputs from the L5 dorsal root. Cell 17–02–2012e33 from Table 2. *A*, voltage-clamp recordings at a holding potential of −70 mV. The root was first stimulated with a 50 μs pulse of increasing amplitude. A low-threshold short-latency IPSC (LT-SL-IPSC) appeared at 10 μA and 20 μA. At 40 μA, the IPSC is followed by a higher-threshold monosynaptic Aδ fibre-mediated EPSC (Aδ-EPSC). The conduction velocity of the fibres conveying the Aδ fibre-mediated EPSC (0.6 m/s) was in the range of slow Aδ afferents (Pinto *et al.* 2008*a*). Stimulation of the same root with a 1 ms pulse additionally evoked a monosynaptic C fibre-driven EPSC (C-EPSC). *B*, latency distribution in low-threshold short-latency IPSC ($n = 20$). Bin width: 1 ms. The IPSC was evoked by saturating pulses of both 50 μs and 1 ms. The histogram was constructed for the fastest IPSC component (see *C*). *C*, analysis of the rising phase of the short-latency IPSC at higher time resolution revealed at least two components which could be activated together (1 + 2) or separately (1 and 2). *D*, schematic of primary afferent inputs to this lamina I neurone. The intercalated neurone (IN) inhibits the lamina I neurone via multiple axodendritic pathways (Santos *et al.* 2009; Luz *et al.* 2010). *E*, current-clamp recordings from the same LCN. The root was stimulated to recruit Aδ fibres. The low-threshold short-latency IPSP (LT-SL-IPSP) preceded the Aδ fibre-driven EPSP (Aδ-EPSP) and prevented spike initiation at low stimulation intensities. Dashed lines: 0 mV. The moment of stimulation is indicated by open arrowheads in all traces.

Low-threshold short-latency disynaptic inhibition

In four LCNs and three PNs a low-threshold short-latency IPSC was evoked by stimulating one or both dorsal roots (L4, $n = 3$; L5, $n = 6$) (Table 2). Recordings from an LCN receiving this type of inhibition from the L5 root are shown in Fig. 2 (cell 17–02–2012e33 from Table 2).

Root stimulation with a 50 μs pulse of increasing amplitude first evoked a low-threshold (10 μA and 20 μA) IPSC (Fig. 2*A*). The monosynaptic Aδ fibre-driven EPSC had a higher threshold (40 μA) and longer latency. The short-latency IPSC had the low failure rate (three in 23 episodes), short latency (mean = 6.7 ms, $n = 20$) (Fig. 2*B*) and small latency variation (S.D., 0.51 ms, $n = 20$) implying a disynaptic nature of the inhibition caused by transmitter release from an intercalated neurone reliably firing upon primary afferent stimulation. The lower border of the CV estimated for the primary afferents conveying this short-latency IPSC was 2.6 m/s (Aδ fibre range) (Pinto *et al.* 2008*a*).

On the rising phase of the short-latency IPSC, several components that were activated together or separately could be distinguished (Fig. 2*C*), suggesting that the intercalated neurone inhibited this lamina I neurone via multiple axodendritic pathways (Fig. 2*D*) (see Luz *et al.* 2010). It is also possible, however, that several inhibitory neurones receiving direct low-threshold primary afferent input might synapse on this lamina I neurone. It should be noted that the failure rates and latency variations presented in Table 2 for all nine cases of low-threshold short-latency inhibition were calculated for the fastest IPSC component.

The functional significance of this type of inhibition became evident in current-clamp experiments (Fig. 2*E*). At weak stimulations, the low-threshold short-latency IPSP hyperpolarized membrane and shunted the monosynaptic Aδ fibre-mediated EPSP. As a result, stronger stimulations were needed to evoke a spike. Thus, this disynaptic inhibition regulated the threshold of lamina I neurone firing upon primary afferent stimulation.

Low-threshold long-latency inhibition

In four PNs a low-threshold long-latency IPSC was evoked by L4 root stimulation (Fig. 3, Table 2). A 50 μs stimulation of increasing amplitude first evoked a polysynaptic IPSC with a long latency (~20 ms), for which the number of intercalated neurones could not be determined. The threshold for the monosynaptic short-latency Aδ fibre-driven EPSC was higher. The root stimulation with a 1 ms pulse also evoked a monosynaptic C fibre-driven EPSC. Holding the PN at −80 mV minimized the low-threshold IPSC and unmasked a longer-latency Aδ fibre-mediated EPSC component (Aδ-EPSC*) that followed the very stable monosynaptic short-latency Aδ fibre-driven EPSC (Fig. 3*B*, left) and preceded the C fibre-driven EPSC (Fig. 3*B*, right).

The role of low-threshold long-latency inhibition was studied in current-clamp mode. The root stimulation recruiting Aδ fibres evoked a spike triggered by the monosynaptic short-latency Aδ fibre-mediated EPSP, whereas the longer-latency Aδ fibre-driven EPSP was shunted by the low-threshold IPSP (Fig. 3*C*, left). At a 1 ms stimulation, the short-latency Aδ fibre-driven EPSP again reliably evoked spikes, whereas the C fibre-mediated EPSP was, in many cases, shunted by the IPSP (Fig. 3*C*, right).

Thus, the low-threshold long-latency IPSP did not interfere with the monosynaptic short-latency Aδ fibre-mediated EPSP, allowing reliable time-locked spike initiation, but controlled and could shunt the longer-latency or polysynaptic Aδ fibre-mediated EPSP and monosynaptic C fibre-mediated EPSP.

A complex interplay of excitatory and inhibitory afferent-driven inputs was able to determine a temporal pattern of spike firing in lamina I neurones (Fig. 4). In one spinal cord, we performed current-clamp recordings of L4 and L5 root-driven inputs first in a PN of the lateral collateral type (red) and then in an LCN (blue). Both neurones were from the same segment (L4), but were not synaptically connected. When the L4 and L5 roots were stimulated with a 1 ms pulse of saturating strength, the Aδ fibre-mediated EPSP evoked firing in the PN. In the LCN, however, the Aδ fibre-mediated EPSP was shunted by an IPSP and the spikes were reliably evoked by the C fibre-mediated EPSP. Thus, afferent-driven inhibition can shape the temporal discharge patterns of lamina I neurones and contribute to complex mechanisms of sensory encoding in the superficial dorsal horn network.

GABA- and glycinergic nature of afferent-driven inhibition

We tested the effects of GABA and glycine receptor blockers on low-threshold IPSCs elicited by stimulating dorsal roots ($n = 7$). Both picrotoxin (100 μM) and strychnine (1 μM) had complex effects suppressing IPSCs and additionally disinhibiting some excitatory inputs similar to those described by Torsney & MacDermott (2006). When picrotoxin was applied first ($n = 5$), both complete ($n = 2$; not shown) and partial ($n = 3$) (Fig. 5*A*) IPSC blocks were achieved. In the case of partial block, an addition of strychnine abolished the IPSC completely and also disinhibited new excitatory inputs (Fig. 5*A*). When strychnine was applied first ($n = 2$), the IPSC block was incomplete (Fig. 5*B*) and the remaining part was suppressed by adding picrotoxin (not shown). The IPSC reversal potential measured for the low-threshold inputs

($n = 8$) was around −80 mV (Fig. 5*C*). Thus, we concluded that the low-threshold afferent-driven inhibition of lamina I LCNs and PNs was mediated via both GABA- and glycinergic synapses.

Local inputs to LCNs

Local inputs to PNs have been described previously (Luz *et al.* 2010). In the present study, we recorded the monosynaptic inputs to lamina I LCNs from both lamina I and lamina II neurones.

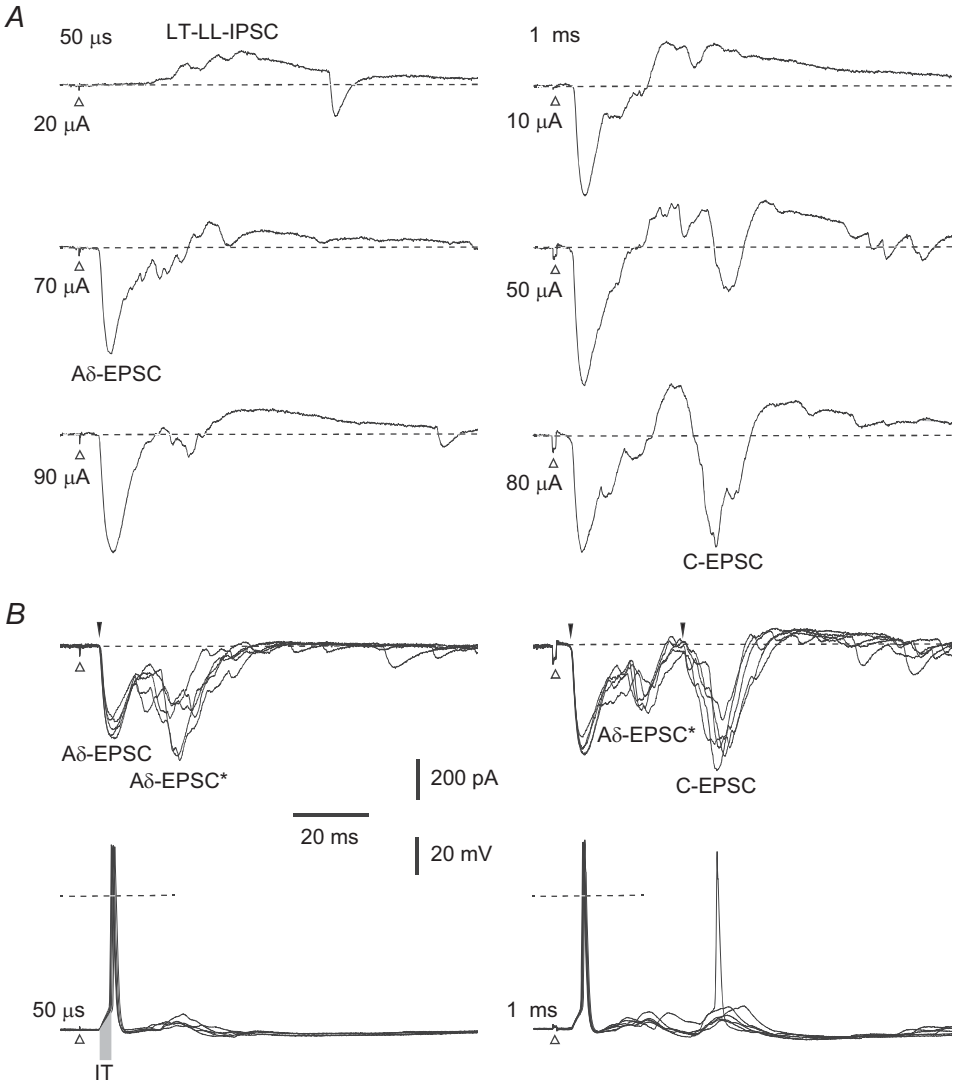

Figure 3. Low-threshold long-latency afferent-driven inhibition
Recordings from a projection neurone (PN) located in segment L4 receiving inputs from the L4 root. *A*, voltage-clamp recordings at −70 mV. When the root was stimulated with 50 μs pulses, a low-threshold long-latency IPSC (LT-LL-IPSC) appeared first (at 20 μA). A short-latency monosynaptic Aδ fibre-mediated EPSC (Aδ-EPSC) had a substantially higher threshold (70 μA). Root stimulation with 1 ms pulses additionally evoked a monosynaptic C fibre-driven EPSC (C-EPSC). *B*, voltage-clamp recordings at −80 mV ($E_{Cl} = -82$ mV) minimized the IPSC and unmasked a longer-latency Aδ fibre-mediated EPSC component (Aδ-EPSC*) following the very stable short-latency monosynaptic Aδ fibre-driven EPSC. Identified monosynaptic Aδ and C fibre-driven EPSCs are indicated by filled arrowheads. *C*, current-clamp recordings from the same PN. The root stimulation recruiting Aδ fibres (left) evoked a spike triggered by the short-latency monosynaptic Aδ fibre-mediated EPSP, whereas the longer-latency Aδ fibre EPSP was shunted by the low-threshold IPSP. At a 1 ms stimulation (right), the short-latency Aδ fibre-mediated EPSP reliably evoked spikes, whereas the C fibre EPSP was in most cases shunted by the low-threshold long-latency IPSP. Dashed lines: 0 mV. Initiation time (IT) of the spike by a strong synaptic input was measured as indicated by the grey bar on the left trace (2.8 ± 0.2 ms, range: 1.6–6.4 ms; $n = 20$). Note a reliable time-locked spike initiation. Data refer to cell 29–02–2012e32 in Table 2.

For 12 LCNs (six rhythmic, four tonic, two unclassified) we found presynaptic excitatory neurones in lamina I (by testing 85 cells). The connection with a postsynaptic rhythmic LCN is shown in Fig. 6*A*. The neurones were directly connected via at least two active synapses, as judged from the two-component rising phase of the monosynaptic EPSC (inset; see also Santos *et al.* 2009). In addition, a large disynaptic EPSC with a varying latency was generated via an intercalated neurone (Luz *et al.* 2010). In current-clamp mode, the LCN was hyperpolarized to −70 mV to stop intrinsic firing and the presynaptic neurone was stimulated to elicit EPSPs. The monosynaptic EPSP summated with the disynaptic EPSP, resulting in a spike discharge.

Of the 12 LCNs with monosynaptic inputs from other lamina I neurones, nine received multiple- and three received single-synapse contacts. Three of the LCNs with multiple-synapse direct inputs also showed a disynaptic input via an intercalated neurone. The efficacy of the EPSPs in evoking spikes was tested for four postsynaptic LCNs that were not rhythmically firing; evoked EPSPs were sub- and suprathreshold in three and one cases, respectively.

For seven LCNs (four rhythmic, three tonic), we recorded monosynaptic inputs (six excitatory, one inhibitory) from lamina II interneurones. Of excitatory inputs, one was a single-synapse connection (Fig. 6*Ba*) and the remaining five were directly wired via multiple synapses and in one case also via an intercalated neurone (not shown). In two LCNs that did not show intrinsic rhythmic firing, the evoked EPSPs were subthreshold. The inhibitory monosynaptic input to an LCN (Fig. 6*Bb*) was a two-component IPSC, indicating that an axon of an inhibitory interneurone may also form multiple direct contacts with the soma and dendrites of an LCN.

Responses to substance P

Both LCNs ($n = 41$) and PNs ($n = 31$) were tested for their sensitivity to substance P (1 μM). In voltage-clamp mode (Fig. 7*A*), the bath application of substance P activated inward currents in 10 of 25 LCNs (40%) and 15 of 21 PNs (71%). In current-clamp mode (Fig. 7*B*), a membrane depolarization was evoked in five of 16 LCNs (31%) and

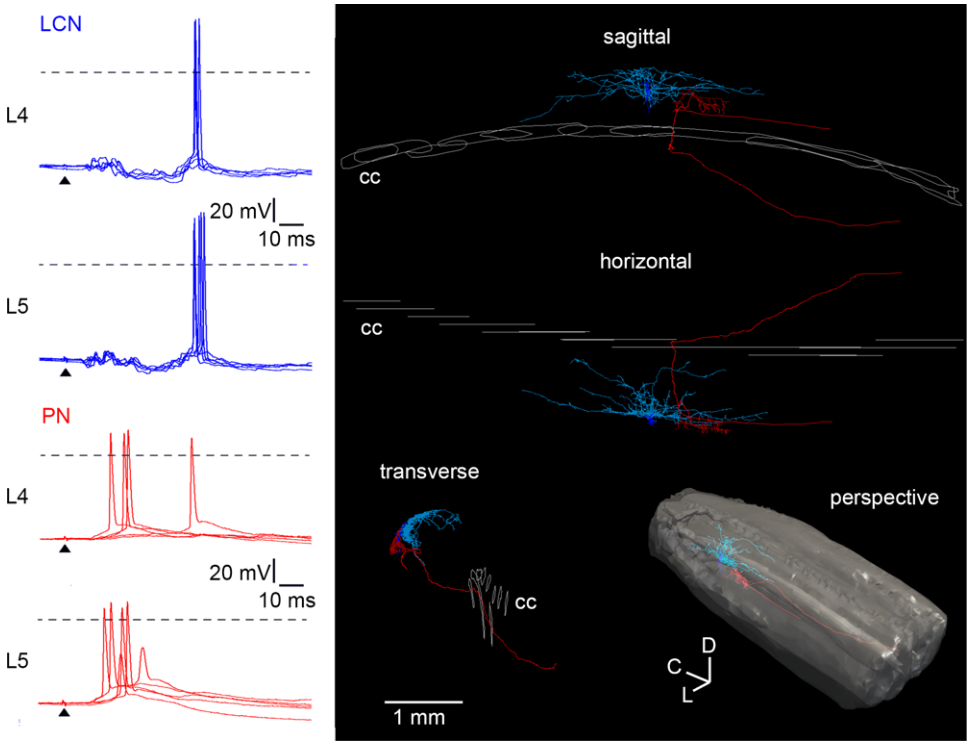

Figure 4. Temporal encoding of spike firing in lamina I neurones
Current-clamp recordings of the L4 and L5 dorsal root-driven inputs in a local-circuit neurone (LCN) (blue) and a projection neurone (PN) (red) located in the L4 segment of one spinal cord. Five consecutive traces are shown superimposed. Anatomical reconstruction did not reveal synaptic contacts between these cells. Roots were stimulated with a 1 ms pulse of saturating strength. Arrowheads indicate the moment of stimulation. Dashed lines: 0 mV. On the 3-D reconstruction: cc, central canal; c, caudal; d, dorsal; l, lateral.

six of 10 PNs (60%). Table 1 gives the numbers of lamina I neurones with different patterns of intrinsic firing that responded to substance P application in either voltage- or current-clamp mode. Thus, both LCNs and PNs could be excited by substance P, although the percentage of responding PNs was higher.

Discussion

The major findings of this study are that lamina I LCNs and PNs: (i) exhibit diverse patterns of intrinsic firing, including a rhythmic discharge in LCNs; (ii) can be inhibited by low-threshold afferent stimulation, and (iii) can be excited by substance P. In addition, LCNs receive monosynaptic inputs from the neurones residing in laminae I and II.

Intrinsic firing properties of LCNs and PNs

The basic firing patterns observed in the present study were similar to those described for lamina I neurones by other groups (Grudt & Perl, 2002; Prescott & De Koninck, 2002; Ruscheweyh *et al.* 2004; Li & Baccei, 2011); however, they were differently represented in the LCNs and PNs in our sample. An interesting finding was the occurrence of an intrinsic rhythmic discharge in almost half of LCNs, which persisted in the presence of synaptic transmission blockers. We did not observe the calcium-dependent oscillatory burst patterns described for lamina I neurones in newborn (P2–P3) animals (Li & Baccei, 2011) because LCNs in our study were more mature (P14–P21) and recorded with internal solutions containing calcium buffers. If we assume that rhythmic LCNs may be both excitatory and inhibitory (Li & Baccei, 2011), they may be critically important for the generation of spontaneous network activity in the dorsal horn (Sandkuhler & Eblen-Zajjur, 1994). In about one-third of LCNs, tonic firing was elicited by a depolarizing current injection. Some LCNs also exhibited gap firing, which has been previously considered as a characteristic feature of lamina I PNs (Ruscheweyh *et al.* 2004) and was also observed in lamina II interneurones (Heinke *et al.* 2004; Yasaka *et al.* 2010). The predominant firing pattern of the PNs in our sample was tonic. Some PNs showed burst firing as described previously in neurones projecting to the periaqueductal grey (Ruscheweyh *et al.* 2004). It should be noted that we did not reveal any spontaneous rhythmic activity in PNs, which suggests that such behaviour in these cells may be restricted to those in newborn animals (Li & Baccei, 2011).

The differences in the distributions of firing patterns between LCNs and PNs reported in this and other studies may have two explanations. Firstly, it is likely that recordings were made in different populations of both LCNs and PNs. In isolated spinal cord, we selected large lamina I neurones, which are found less frequently in spinal cord slices. It should also be noted that our cells were located in the lateral part of lamina I. The lateral superficial dorsal horn receives cutaneous inputs from the proximal skin areas (in the L4 segment of the rat spinal cord) from the surface of the foot, leg and, in the most lateral part, from the thigh and hip (Brown, 1982; Woolf & Fitzgerald, 1986). Secondly, the firing behaviour of a dorsal horn neurone depends on how efficiently the voltage-gated conductances, which are mainly expressed in the axon (Safronov *et al.* 1997; Safronov, 1999), drive the large capacitive load of the dendritic membrane. As evidenced by our reconstructions, both the axon and dendrites of LCNs and PNs are preserved to a considerably larger degree in the spinal cord preparation (Luz *et al.* 2010; Szucs *et al.* 2010, 2013). Thus, more recordings from identified lamina I neurones will be necessary to elucidate the cell-specific distributions of firing properties. Nevertheless, existing data indicate that the diverse firing properties of superficial dorsal horn neurones determine how synaptic excitation is converted into trains of action potentials (Lopez-Garcia & King,

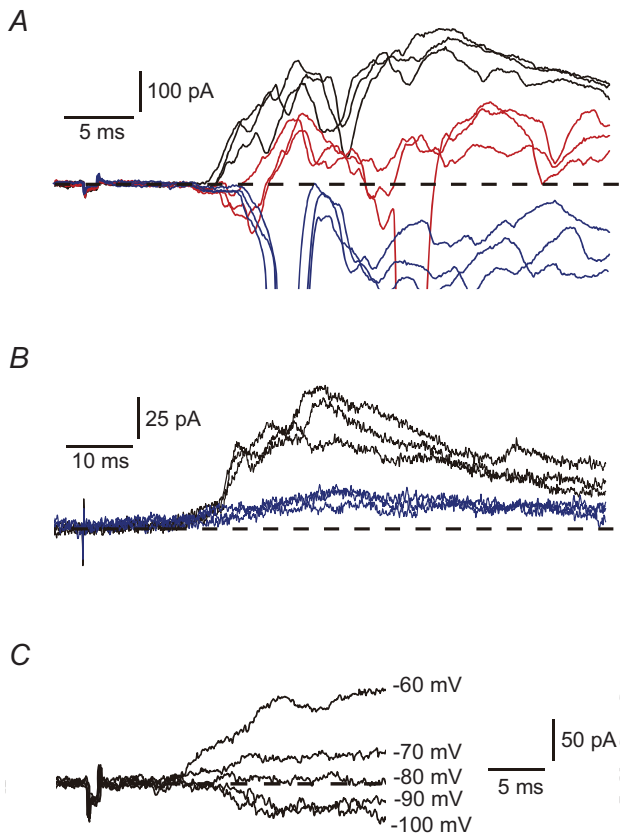

Figure 5. Pharmacology and inversion of afferent-driven IPSCs
A, IPSCs in control (black), in 100 μM picrotoxin (red) and after addition of 1 μM strychnine (blue). Potential: −70 mV. *B*, IPSCs in control (black) and in 1 μM strychnine (blue). *C*, an IPSC at different membrane potentials.

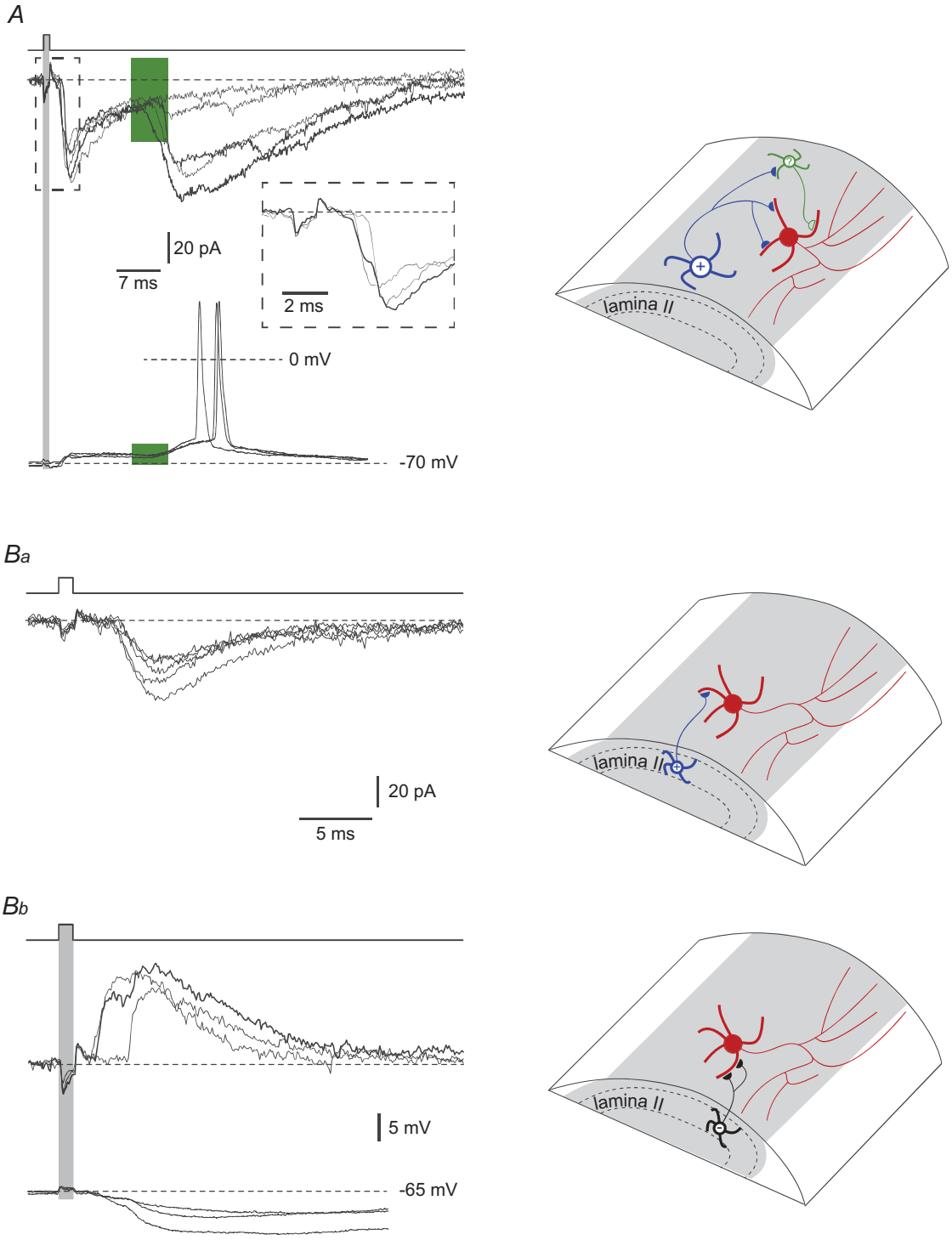

Figure 6. Local inputs to local-circuit neurones (LCNs) from laminae I and II
A, EPSCs evoked in an LCN by stimulating another lamina I neurone. The LCN was voltage-clamped at −80 mV. The short-latency monosynaptic EPSC had two components (inset). The latency variation of the disynaptic EPSC, generated via an intercalated neurone, is indicated in green. In current-clamp mode, this LCN of rhythmic firing type was hyperpolarized to −70 mV to stop intrinsic discharge. Note that the disynaptic EPSP augmented membrane depolarization induced by the monosynaptic EPSP. *Ba*, a single-synapse excitatory input to an LCN from a lamina II excitatory interneurone. Consecutive EPSCs ($n = 5$) were recorded at −80 mV. *Bb*, monosynaptic input to an LCN from a lamina II inhibitory interneurone. The inhibitory interneurone formed two direct synapses on the LCN as judged from the two components on the rising phase of the IPSC recorded at −60 mV. In current-clamp mode, the two-component monosynaptic IPSP was evoked by stimulating the same presynaptic neurone.

1994; Graham *et al.* 2004) and may set rhythmic network activity in developing spinal cord (Li & Baccei, 2011).

Low-threshold afferent-driven inhibition: a new gate controlling pain?

The functional significance of the low-threshold afferent-driven inhibition of LCNs and PNs described here can be considered from several points of view. Firstly, the present data provide experimental evidence for the existence of a postsynaptic gate mechanism, which was missing from the original theory of pain control (Melzack & Wall, 1965). Our results suggest that low-threshold non-noxious peripheral afferents can inhibit, via one intercalated neurone, a PN and therefore larger noxious afferent input is required to reach the firing threshold. This simple postsynaptic mechanism can also explain the phenomenon of pain control by innocuous cutaneous stimulation (Willis & Coggeshall, 1991). Secondly, disinhibition of this pathway may cause hyperalgesia. A decrease in the afferent-driven inhibition of lamina I PNs or LCNs will obviously lower the firing threshold for the nociceptive Aδ or C fibre inputs. Thirdly, it has been shown that low-threshold afferents can project to lamina I neurones via polysynaptic excitatory pathways, which are suppressed under normal conditions by intrinsic inhibitory circuitries, but can open in the presence of glycine and GABA receptor blockers (Torsney & MacDermott, 2006), causing allodynia (Yaksh, 1989). It is therefore possible that the direct inhibitory link described here represents another circuitry serving to uncouple the nociceptive specific PNs from low-threshold afferent excitatory inputs and prevent or reduce allodynia. Fourthly, the afferent-driven inhibition may be critical for the generation of spatiotemporal patterns of activity in lamina I (see Fig. 4).

Studies carried out using spinal cord slice preparation observed excitatory Aδ and C fibre-mediated inputs to lamina I neurones (Grudt & Perl, 2002; Dahlhaus *et al.* 2005; Torsney & MacDermott, 2006; Vikman *et al.* 2008). However, to our knowledge, there are no available reports on low-threshold afferent-driven inhibitory inputs. One can assume therefore that their detection might critically rely on the preservation of long axonal pathways, as in the preparation we used. In agreement with this, many short-latency inhibitory inputs to the LCNs and PNs located in segment L4 were mediated by the afferents entering via the L5 dorsal root. Furthermore, inhibition of some superficial dorsal horn neurones by cutaneous stimulation could be evoked in the rat spinal cord–hind limb preparation (Lopez-Garcia & King, 1994) and in an *in vivo* preparation of adult mouse spinal cord (Graham *et al.* 2004).

The low failure rate and small latency variation of IPSCs indicated that the low-threshold short-latency afferent-driven inhibition was disynaptic. Disynaptic GABA- and glycine-mediated inhibition, which followed excitation, was observed in the substantia gelatinosa neurones (Yoshimura & Nishi, 1995). Although our experiments did not address the issue of the laminar location of the intercalated neurone, several of its important features have been revealed. This should be a GABA- and/or glycinergic neurone with dendrites that receive direct input from low-threshold afferents. The latter should be strong enough to reliably evoke action potentials with little variation in initiation time. The intercalated neurone should also be wired to a lamina I neurone

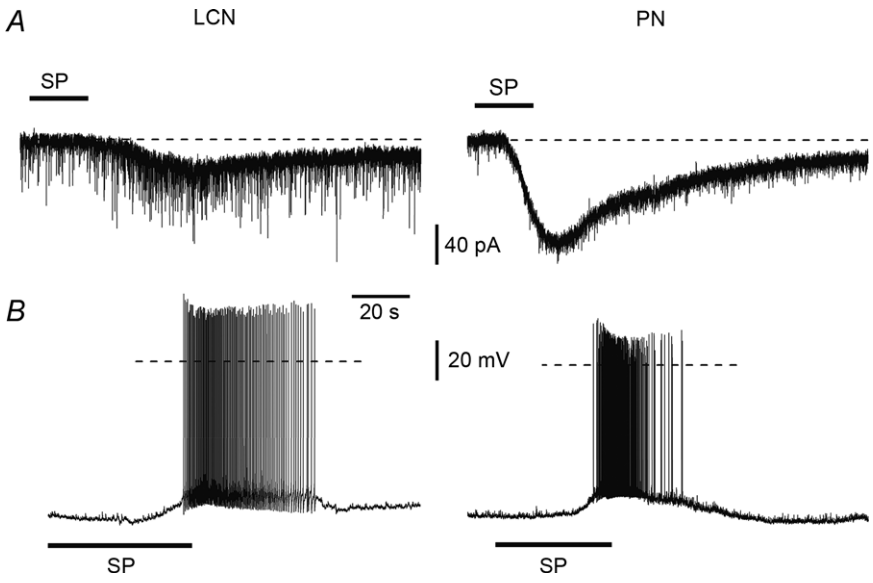

Figure 7. Responses to 1 μM substance P
A, voltage-clamp recordings at −80 mV of currents induced by substance P (SP) application in a local-circuit neurone (LCN) and a projection neurone (PN). *B*, current-clamp recordings from another LCN and another PN. Dashed line: 0 mV.

via the short axodendritic pathways (Luz *et al.* 2010) required for the induction of a short-latency inhibition. Furthermore, transmitter release is likely to occur in multiple synapses, thus increasing the overall inhibitory effect.

The stimulation required to evoke the disynaptic inhibition in the present study (10–20 μA; 50 μs) was within the range used for Aβ fibre activation by Torsney & MacDermott (2006) and Pinto *et al.* (2008*a*) and was subthreshold for the monosynaptic Aδ fibre inputs. Although the estimated CV of the conveying afferents did not reach the Aβ range (>4.2 m/s; Pinto *et al.* 2008*a*), this might result, at least in some cases, from the underestimation of conduction delay on the intercalated neurone (at 22–24°C). The action potential initiation time in the intercalated neurone might be considerably longer than the 2 ms observed in our fastest neurones. Thus, disynaptic inhibition is likely to be mediated via Aβ afferents or via low-threshold mechanical Aδ afferents innervating hair follicles, which represent about one-third of the Aδ afferent population (Koltzenburg *et al.* 1997; Djouhri *et al.* 1998). By contrast, monosynaptic excitatory inputs, which followed short-latency inhibition, were mediated via slower-conducting high-threshold Aδ and C afferents.

LCNs: local inputs and substance P responses

Lamina I neurones are important elements of the intrinsic superficial dorsal horn network (Graham *et al.* 2007; Santos *et al.* 2007, 2009; Kato *et al.* 2009; Todd, 2010). LCNs have an axon, which branches densely within the ipsilateral dorsal horn and may spread for several segments (Szucs *et al.* 2013), forming synapses on PNs (Luz *et al.* 2010). Here, we also show that LCNs can receive numerous inputs from other lamina I neurones, as well as from lamina II neurones. Inhibitory LCNs (Todd & Sullivan, 1990; Szucs *et al.* 2013) may convey afferent-driven inhibition of PNs. Thus, LCNs make an important contribution to neuronal interconnectivity in lamina I.

As PNs in lamina I are much less numerous (~5%) (Spike *et al.* 2003; Todd & Koerber, 2006) than NK1R-expressing neurones (~45%) (Todd *et al.* 1998), the majority of the latter should be LCNs. LCNs show weak staining for NK1R (Cheunsuang & Morris, 2000; Al Ghamdi *et al.* 2009); however, as we found here, about one-third of them show physiological responses to substance P application. NK1R-expressing neurones are likely to be excitatory (Littlewood *et al.* 1995). Thus, substance P release from the nociceptive primary afferents following noxious stimulation (Duggan *et al.* 1987; Mantyh *et al.* 1995) may act on the PNs in two ways: directly, and via excitatory LCNs expressing NK1Rs. This mechanism may increase the overall excitation of nociceptive PNs.

In conclusion, the firing behaviour, afferent-driven inhibition, intralaminar connectivity and substance P sensitivity of lamina I LCNs and PNs described here can play important roles in spinal nociceptive processing.

References

Al-Khater KM, Kerr R & Todd AJ (2008). A quantitative study of spinothalamic neurons in laminae I, III, and IV in lumbar and cervical segments of the rat spinal cord. *J Comp Neurol* **511**, 1–18.

Al Ghamdi KS, Polgar E & Todd AJ (2009). Soma size distinguishes projection neurons from neurokinin 1 receptor-expressing interneurons in lamina I of the rat lumbar spinal dorsal horn. *Neuroscience* **164**, 1794–1804.

Bice TN & Beal JA (1997). Quantitative and neurogenic analysis of the total population and subpopulations of neurons defined by axon projection in the superficial dorsal horn of the rat lumbar spinal cord. *J Comp Neurol* **388**, 550–564.

Brown AG (1982). The dorsal horn of the spinal cord. *Q J Exp Physiol* **67**, 193–212.

Cheunsuang O & Morris R (2000). Spinal lamina I neurons that express neurokinin 1 receptors: morphological analysis. *Neuroscience* **97**, 335–345.

Dahlhaus A, Ruscheweyh R & Sandkuhler J (2005). Synaptic input of rat spinal lamina I projection and unidentified neurones *in vitro*. *J Physiol* **566**, 355–368.

Djouhri L, Bleazard L & Lawson SN (1998). Association of somatic action potential shape with sensory receptive properties in guinea-pig dorsal root ganglion neurones. *J Physiol* **513**, 857–872.

Duggan AW, Morton CR, Zhao ZQ & Hendry IA (1987). Noxious heating of the skin releases immunoreactive substance P in the substantia gelatinosa of the cat: a study with antibody microprobes. *Brain Res* **403**, 345–349.

Graham BA, Brichta AM & Callister RJ (2004). In vivo responses of mouse superficial dorsal horn neurones to both current injection and peripheral cutaneous stimulation. *J Physiol* **561**, 749–763.

Graham BA, Brichta AM & Callister RJ (2007). Moving from an averaged to specific view of spinal cord pain processing circuits. *J Neurophysiol* **98**, 1057–1063.

Grudt TJ & Perl ER (2002). Correlations between neuronal morphology and electrophysiological features in the rodent superficial dorsal horn. *J Physiol* **540**, 189–207.

Heinke B, Ruscheweyh R, Forsthuber L, Wunderbaldinger G & Sandkuhler J (2004). Physiological, neurochemical and morphological properties of a subgroup of GABAergic spinal lamina II neurones identified by expression of green fluorescent protein in mice. *J Physiol* **560**, 249–266.

Kato G, Kawasaki Y, Koga K, Uta D, Kosugi M, Yasaka T, Yoshimura M, Ji RR & Strassman AM (2009). Organization of intralaminar and translaminar neuronal connectivity in the superficial spinal dorsal horn. *J Neurosci* **29**, 5088–5099.

Koltzenburg M, Stucky CL & Lewin GR (1997). Receptive properties of mouse sensory neurons innervating hairy skin. *J Neurophysiol* **78**, 1841–1850.

Li J & Baccei ML (2011). Pacemaker neurons within newborn spinal pain circuits. *J Neurosci* **31**, 9010–9022.

Littlewood NK, Todd AJ, Spike RC, Watt C & Shehab SA (1995). The types of neuron in spinal dorsal horn which possess neurokinin-1 receptors. *Neuroscience* **66**, 597–608.

Lopez-Garcia JA & King AE (1994). Membrane properties of physiologically classified rat dorsal horn neurons *in vitro*: correlation with cutaneous sensory afferent input. *Eur J Neurosci* **6**, 998–1007.

Lu Y & Perl ER (2005). Modular organization of excitatory circuits between neurons of the spinal superficial dorsal horn (laminae I and II). *J Neurosci* **25**, 3900–3907.

Luz LL, Szucs P, Pinho R & Safronov BV (2010). Monosynaptic excitatory inputs to spinal lamina I anterolateral-tract-projecting neurons from neighbouring lamina I neurons. *J Physiol* **588**, 4489–4505.

Mantyh PW, Allen CJ, Ghilardi JR, Rogers SD, Mantyh CR, Liu H, Basbaum AI, Vigna SR & Maggio JE (1995). Rapid endocytosis of a G protein-coupled receptor: substance P evoked internalization of its receptor in the rat striatum *in vivo*. *Proc Natl Acad Sci U S A* **92**, 2622–2626.

Marshall GE, Shehab SA, Spike RC & Todd AJ (1996). Neurokinin-1 receptors on lumbar spinothalamic neurons in the rat. *Neuroscience* **72**, 255–263.

Melnick IV, Santos SF, Szokol K, Szucs P & Safronov BV (2004). Ionic basis of tonic firing in spinal substantia gelatinosa neurons of rat. *J Neurophysiol* **91**, 646–655.

Melzack R & Wall PD (1965). Pain mechanisms: a new theory. *Science* **150**, 971–979.

Pinto V, Derkach VA & Safronov BV (2008*a*). Role of TTX-sensitive and TTX-resistant sodium channels in Aδ- and C-fibre conduction and synaptic transmission. *J Neurophysiol* **99**, 617–628.

Pinto V, Szucs P, Derkach VA & Safronov BV (2008*b*). Monosynaptic convergence of C- and Aδ-afferent fibres from different segmental dorsal roots on to single substantia gelatinosa neurones in the rat spinal cord. *J Physiol* **586**, 4165–4177.

Pinto V, Szucs P, Lima D & Safronov BV (2010). Multisegmental Aδ- and C-fibre input to neurons in lamina I and the lateral spinal nucleus. *J Neurosci* **30**, 2384–2395.

Prescott SA & De Koninck Y (2002). Four cell types with distinctive membrane properties and morphologies in lamina I of the spinal dorsal horn of the adult rat. *J Physiol* **539**, 817–836.

Ruscheweyh R, Ikeda H, Heinke B & Sandkuhler J (2004). Distinctive membrane and discharge properties of rat spinal lamina I projection neurones *in vitro*. *J Physiol* **555**, 527–543.

Safronov BV (1999). Spatial distribution of Na^+ and K^+ channels in spinal dorsal horn neurones: role of the soma, axon and dendrites in spike generation. *Prog Neurobiol* **59**, 217–241.

Safronov BV, Pinto V & Derkach VA (2007). High-resolution single-cell imaging for functional studies in the whole brain and spinal cord and thick tissue blocks using light-emitting diode illumination. *J Neurosci Methods* **164**, 292–298.

Safronov BV, Wolff M & Vogel W (1997). Functional distribution of three types of Na^+ channel on soma and processes of dorsal horn neurones of rat spinal cord. *J Physiol* **503**, 371–385.

Sandkuhler J & Eblen-Zajjur AA (1994). Identification and characterization of rhythmic nociceptive and non-nociceptive spinal dorsal horn neurons in the rat. *Neuroscience* **61**, 991–1006.

Santos SF, Luz LL, Szucs P, Lima D, Derkach VA & Safronov BV (2009). Transmission efficacy and plasticity in glutamatergic synapses formed by excitatory interneurons of the substantia gelatinosa in the rat spinal cord. *PLoS One* **4**, e8047.

Santos SF, Melnick IV & Safronov BV (2004). Selective postsynaptic inhibition of tonic-firing neurons in substantia gelatinosa by μ-opioid agonist. *Anesthesiology* **101**, 1177–1183.

Santos SF, Rebelo S, Derkach VA & Safronov BV (2007). Excitatory interneurons dominate sensory processing in the spinal substantia gelatinosa of rat. *J Physiol* **581**, 241–254.

Spike RC, Puskar Z, Andrew D & Todd AJ (2003). A quantitative and morphological study of projection neurons in lamina I of the rat lumbar spinal cord. *Eur J Neurosci* **18**, 2433–2448.

Szucs P, Luz LL, Lima D & Safronov BV (2010). Local axon collaterals of lamina I projection neurons in the spinal cord of young rats. *J Comp Neurol* **518**, 2645–2665.

Szucs P, Luz LL, Pinho R, Aguiar P, Antal Z, Tiong SY, Todd AJ & Safronov BV (2013). Axon diversity of lamina I local-circuit neurons in the lumbar spinal cord. *J Comp Neurol* **521**, 2719–2741.

Szucs P, Pinto V & Safronov BV (2009). Advanced technique of infrared LED imaging of unstained cells and intracellular structures in isolated spinal cord, brainstem, ganglia and cerebellum. *J Neurosci Methods* **177**, 369–380.

Todd AJ (2010). Neuronal circuitry for pain processing in the dorsal horn. *Nat Rev Neurosci* **11**, 823–836.

Todd AJ & Koerber R (2006). Neuroanatomical substrates of spinal nociception. In *Wall and Melzack's Textbook of Pain*, 5th edn, eds. McMahon SB & Koltzenburg M, pp. 73–90. Churchill Livingstone, Edinburgh.

Todd AJ, McGill MM & Shehab SA (2000). Neurokinin 1 receptor expression by neurons in laminae I, III and IV of the rat spinal dorsal horn that project to the brainstem. *Eur J Neurosci* **12**, 689–700.

Todd AJ, Spike RC & Polgar E (1998). A quantitative study of neurons which express neurokinin-1 or somatostatin sst_{2a} receptor in rat spinal dorsal horn. *Neuroscience* **85**, 459–473.

Todd AJ & Sullivan AC (1990). Light microscope study of the coexistence of GABA-like and glycine-like immunoreactivities in the spinal cord of the rat. *J Comp Neurol* **296**, 496–505.

Torsney C & MacDermott AB (2006). Disinhibition opens the gate to pathological pain signalling in superficial neurokinin 1 receptor-expressing neurons in rat spinal cord. *J Neurosci* **26**, 1833–1843.

Vikman KS, Rycroft BK & Christie MJ (2008). Switch to Ca^{2+}-permeable AMPA and reduced NR2B NMDA receptor-mediated neurotransmission at dorsal horn nociceptive synapses during inflammatory pain in the rat. *J Physiol* **586**, 515–527.

Willis WD & Coggeshall RE (1991). *Sensory Mechanisms of the Spinal Cord*. John Wiley & Sons, New York, NY.

Woolf CJ & Fitzgerald M (1986). Somatotopic organization of cutaneous afferent terminals and dorsal horn neuronal receptive fields in the superficial and deep laminae of the rat lumbar spinal cord. *J Comp Neurol* **251**, 517–531.

Yaksh TL (1989). Behavioral and autonomic correlates of the tactile evoked allodynia produced by spinal glycine inhibition: effects of modulatory receptor systems and excitatory amino acid antagonists. *Pain* **37**, 111–123.

Yasaka T, Tiong SY, Hughes DI, Riddell JS & Todd AJ (2010). Populations of inhibitory and excitatory interneurons in lamina II of the adult rat spinal dorsal horn revealed by a combined electrophysiological and anatomical approach. *Pain* **151**, 475–488.

Yoshimura M & Nishi S (1995). Primary afferent-evoked glycine- and GABA-mediated IPSPs in substantia gelatinosa neurones in the rat spinal cord *in vitro*. *J Physiol* **482**, 29–38.

Additional information

Competing interests

None declared.

Author contributions

B.V.S. contributed to the conception and design of the experiments, and wrote and revised the paper. All authors contributed to the collection, analysis and interpretation of data, and approved the final manuscript for publication. All experiments were performed in the laboratory of the Neuronal Networks Group, Institute of Molecular and Cellular Biology, University of Porto, Portugal.

Funding

This work was supported by FEDER funds through COMPETE and by national funds through Fundação para a Ciência e a Tecnologia under the project FCOMP-01-0124-FEDER-029623 (PTDC/NEU-SCC/0347/2012 and PTDC/NEU-NMC/0494/2012).

Acknowledgements

None declared.